Josephson-flux depinning in granular $YBa_2Cu_3O_{7-\delta}$

J. Jung
Department of Physics, University of Alberta, Edmonton, Alberta, Canada T6G 2J1

M. A-K. Mohamed
Department of Physics, University of Alberta, Edmonton, Alberta, Canada T6G 2J1
and Department of Physics, University of Lethbridge, Lethbridge, Alberta, Canada T1K 3M4

I. Isaac and L. Friedrich
Department of Physics, University of Alberta, Edmonton, Alberta, Canada T6G 2J1
(Received 23 June 1993; revised manuscript received 1 November 1993)

Josephson- (intergrain-) flux depinning was studied in a Josephson-junction network of granular YBCO and YBCO/Ag superconductors. We measured temperatures and magnetic fields at which the Josephson-flux depinning occurs and analyzed the corresponding relaxation processes. A direct relationship between depinning of the Josephson vortices and dissipation of the transport (Josephson) critical current was found. Special experimental techniques were applied to achieve those objectives, allowing (a) detection of the Josephson-flux motion without the influence of the intragrain (Abrikosov) flux; and (b) direct measurement of changes in the effective activation energy for the Josephson-flux motion and corresponding changes in the Josephson critical current. The results were interpreted in the framework of the models of granular superconductivity developed by Tinkham and Lobb [Solid State Phys. **43**, 91 (1989)], and by Clem [Physica C **153-155**, 50 (1988)]. The results support the idea given in those models, that the pinning barrier for the Josephson-flux motion originates from the variation of the Josephson coupling energy within the junction network.

I. INTRODUCTION

Granularity of bulk high-temperature ceramic superconductors modifies the electromagnetic properties of those materials. Grain boundaries in high-T_c ceramics limit the transport critical current and allow easy penetration of a magnetic field into the superconductor. Attempts to separate the intergranular properties from the intragrain ones led to the picture of high-T_c ceramics as an assembly of grains weakly coupled by Josephson-type links. Studies of the response of zero-field-cooled superconducting ceramics to applied fields[1-4] revealed that, at low magnetic fields up to a certain intergrain field H_{c1j}, grain boundaries are shielded. At higher fields, magnetic field penetrates the grain boundaries in the form of Josephson vortices. Intergrain superconductivity in Josephson links is completely extinguished above a grain-decoupling field H_{c2j}. For a ceramic $YBa_2Cu_3O_{7-\delta}$ (YBCO) at 77 K, for example, it was estimated that H_{c1j} varies between 1 and 10 G, and H_{c2j} has values over a range between 150 and 1000 G.[4] That broad range of values for both H_{c1j} and H_{c2j} is caused by the sample geometry (demagnetization effects) and by varying the Josephson-coupling energy along the grain boundaries. Understanding the basic transport and magnetic properties of the Josephson-junction network in granular superconductors requires knowledge of the relationship between the macroscopic superconducting properties of high-T_c ceramics [such as the transport (Josephson) critical current density and the sample magnetization at low magnetic fields] and the intrinsic properties of grain boundaries, including formation and pinning of the intergrain (Josephson) magnetic vortices. Such information has not been provided by conventional transport and magnetic measurement methods. At magnetic fields higher than a grain-decoupling field H_{c2j}, sample magnetization is essentially dominated by the intragranular flux creep and flow. The suppression of the intragrain critical current density J_c by a magnetic field is believed to arise from either an intrinsic melting of the intragranular flux lattice or a thermally activated depinning of the intragrain vortices.[5-7] The values of the intragrain J_c were found to be associated with the existence of an irreversibility line, which is characterized by temperatures T_{irr} and magnetic fields H_{irr}, above which J_c is essentially zero. In conventional type-II superconductors, H_{irr} and H_{c2} virtually coincide. In high-temperature superconductors, H_{irr} is much lower than H_{c2}. Two main theoretical interpretations of the irreversibility line are that either H_{irr} is the melting field of the intragrain-vortex lattice or it just represents a thermal depinning of the intragrain vortices at high temperatures.[5-7] Weak pinning shifts the irreversibility line toward lower temperatures and may broaden the transition. Irreversibility lines have been investigated in ceramics, thin films, and single crystals for applied magnetic fields up to 15 T using the following measurements: dc magnetization[8] (by determining a temperature T_{irr} at which the zero-field-cooling and field-cooling magnetic moments coincide), the resistivity criterion,[9] I-V curves,[10] the ac penetration depth,[11] and the damping peaks of a vibrating superconducting sample.[12] However, these kinds of experiments have not pro-

vided any information about the intergrain-flux depinning. The main reasons for that are the superposition of an intergranular and intragranular magnetic flux at magnetic fields below the Josephson upper critical field (grain-decoupling field) H_{c2j}, and the low value of that field.

The parameters that are essential for a proper estimation of the transport critical current density J_{cj} in the Josephson-junction network of high-T_c ceramics are the magnetic fields H_{c2j} and temperatures T_{cj} at which superconducting grains are decoupled and J_{cj} drops to zero. Dissipation processes at grain boundaries due to the intergrain-flux motion can be seen in the imaginary part of the ac susceptibility measured as a function of temperature;[13,14] however, its complicated dependence on the frequency and amplitude of the ac field prevents one from establishing a reliable relationship between the grain-decoupling field and temperature. Measurement of the hysteretic behavior of the magnetization for a ceramic sample does not allow for precise determination of H_{c2j}, due to superposition of the intergrain and intragrain hysteresis loops.[1] On the other hand, the superconducting grains in high-T_c ceramics are believed to be connected not only by Josephson-type weak links but also by non-weakly-linked continuous microbridges, which have the intrinsic properties of the grain-forming material.[15] These microbridges, which constitute about 0.01–0.1 % of the grain-boundary area available for the current, are responsible for the presence of the transport supercurrent up to very high magnetic fields (5–10 T). This prevents in practice the estimation of H_{c2j} for the weakly linked parts of grain boundaries from measurements of the transport critical current density as a function of applied magnetic field, using the standard four-probe technique.

The rapid drop in J_{cj} at very low magnetic fields is caused by decoupling of the Josephson weak links at grain boundaries in bulk ceramic samples. According to the Josephson weak-link model, the decoupling field H_{c2j} for the weak links is given by[15,16]

$$H_{c2j}=\frac{\Phi_0}{\langle D\rangle 2\lambda} ,$$

where Φ_0 is the flux quantum, λ is the penetration depth, and $\langle D\rangle$ is the average grain size in the direction mutually perpendicular to the applied current and magnetic field. The temperature dependence of H_{c2j} in this formula is governed by that of λ. Motion of the intergrain vortices along the grain boundaries will reduce the transport critical current density and consequently the temperature and magnetic field at which the grains become decoupled. The critical values of temperature and magnetic field at which the transport critical current density is zero separate two regimes which determine the transport properties of superconducting ceramics; the intergrain-(Josephson-) flux pinning and intergrain-flux flow regimes. The intergrain-flux-pinning–flux-flow line drawn on a (H,T) diagram is characterized by temperatures and magnetic fields below those corresponding to the intragrain "irreversibility" line. The problem is to determine temperatures and magnetic fields that pinpoint the intergrain flux-pinning–flux-flow critical line and to compare them with temperatures and fields at which the intergrain (transport) current J_{cj} drops to zero.

Studies of dc superconducting quantum interference device (SQUID) magnetization in superconducting ceramics and powers[17] revealed that fast cooling of YBCO ceramics in a magnetic field causes more intergrain- (Josephson-) flux trapping than slow (equilibrium) cooling. During subsequent warming, that additional flux depins at a certain temperature whose value depends on the magnetic field. This simple procedure provided us with the means to detect the intergrain-flux trapping effects without the influence of the intragrain flux, to determine temperatures and fields at which the intergrain vortices depin, and to investigate the corresponding relaxation effects.

On the other hand, we developed a technique[18] to measure the intergrain (Josephson) critical current and its dissipation due to the Josephson-flux motion. This method employs a self-sustaining (persistent) supercurrent flowing in a ceramic superconducting ring and a contactless detection of the critical value of the persistent current and its dissipation. Changes in the magnetic field generated by the current were measured with a scanning Hall-probe system.

In this paper, we present the results of studies of the intergrain-flux motion in YBCO and YBCO/Ag granular superconductors, and measurements of the intergrain critical current and its dissipation as a function of temperature, using the methods described above. The leading idea of these investigations was to determine the physical properties of the Josephson-junction network in granular high-T_c superconductors, namely:

(a) The temperatures, magnetic fields, and relaxation effects which characterize the Josephson-vortex depinning, and their dependence on the inhomogeneity of the Josephson-coupling energy within the junction network;

(b) The dissipation rate of the Josephson critical current and its relationship to the Josephson-vortex motion.

II. EXPERIMENTAL PROCEDURE

We measured changes in the dc magnetic moment as a function of temperature for various applied magnetic fields (over a range between 0 and 2000 G) in field-cooled samples of YBCO and YBCO/Ag (2 wt % and 4 wt %) ceramics. Those measurements were done in a Quantum Design SQUID magnetometer. The measurements of the Meissner field and transport critical currents were performed on samples of a YBCO/Ag (2 wt %) composite using a Hall-probe system.

A. Sample preparation

Ceramic samples were prepared using $YBa_2Cu_3O_{7-\delta}$ obtained by the standard solid-state reaction technique from powders of high-purity compounds: Y_2O_3, CuO,

and $BaCO_3$. The powders were calcined in an atmosphere of flowing pure oxygen for 24 h at 925 °C. The resulting product was then pulverized and used to form (under a pressure of about 7000 bar) cylinder-shaped and disk-shaped samples for further studies. Those samples were sintered in flowing oxygen at 925–930 °C for 7 h and cooled at variable rates down to room temperature (3 °C/min between 925 and 700 °C and 1 °C/min below 700 °C). In the case of YBCO/Ag composites, silver powder was added to YBCO before the sintering process. Cylinder-shaped samples that were produced in this way were about 4.5 mm in diameter and 8–11 mm in length. Disk-shaped samples had a diameter of 16 mm, and were 3.0–3.5 mm thick. A 6-mm-diam hole was then drilled in the disk center (using a diamond tube-shaped drill sprayed with water) in order to manufacture two samples: a ring-shaped sample for critical-current studies, and an inner piece, a pellet of 4.5 mm diameter, for the magnetization measurements. The latter measurements were done on six samples: ceramic YBCO cylinder-shaped samples (YBCO nos. 1 and 2), and pellets cut from YBCO, YBCO/Ag (2 wt %), and YBCO/Ag (4 wt %) ceramic disks [YBCO no. 3, YBCO/Ag (2 wt %) nos. 1 and 2, YBCO/Ag (4 wt %)].

B. Description of the measurement method

Special procedures were applied to measure the dependence of the intergrain-magnetic-flux trapping and its expulsion on temperature for YBCO and YBCO/Ag ceramic samples. Two different experimental techniques have been used: (1) the measurement of dc magnetic moment using a SQUID magnetometry, and (2) the measurement of the magnetic-field profile above a superconducting sample using a scanning Hall-probe system. When a ceramic YBCO superconductor is cooled slowly down in a small magnetic field starting at a temperature above T_c, the Meissner currents cause partial expulsion of a magnetic field that penetrated the sample at temperatures above T_c [Fig. 1(a)]. The remaining field is trapped at the grain boundaries (intergrain flux) and inside the grains (intragrain flux). Fast cooling of the same sample in a magnetic field down to low temperature (e.g., 10 K) results in an additional nonequilibrium magnetic-flux trapping and a reduced Meissner expulsion [Fig. 1(b)]. Subsequent warming of the sample causes an expulsion of this additional flux at temperatures close to T_c [Figs. 1(b) and 1(c)]. Those experiments were repeated for a pressed-powder YBCO sample which was formed after pulverizing the ceramic one. It was found that fast and slow cooling of this powder sample does not produce the same effects as cooling of the ceramic YBCO superconductor (Fig. 2). This provided strong evidence that the additional magnetic flux trapped in the ceramic YBCO during the fast cooling procedure is of an intergrain nature. The measurements of the sample magnetic moment (in a SQUID magnetometer) were performed during cooling, for the slow cooling procedure (using a cooling rate of about 0.05–0.1 K/min), and during warming (with a rate of about 0.1–0.5 K/min) after the fast cooling procedure down to 10 K (using a cooling rate of about 3–4 K/min at temperatures between 100 and 10 K).

Trapping the intergrain flux during fast cooling and its depinning during warming were also detected by the Hall-probe system, which was used to measure magnetic-flux trapping and its expulsion across a super-

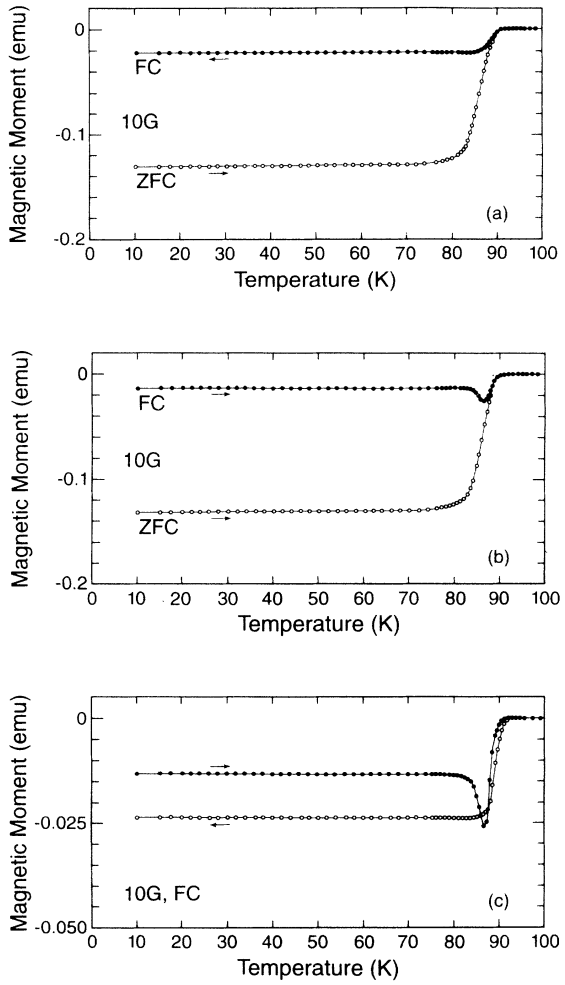

FIG. 1. Dependence of the field-cooled (FC) and zero-field-cooled (ZFC) magnetic moments at 10 G on temperature measured for ceramic YBCO no. 1 (a rod-shaped sample of 4.5 mm in diameter and 10.7 mm in length). The magnetic field was applied along the axis of the rod. The arrows indicate the temperature change during the measurements (warming or cooling). The lines provide a guide for the eye. (a) The field-cooled moment measured during slow equilibrium cooling with an average rate of 0.05–0.1 K/min (solid circles); open circles mark the zero-field-cooled moment measured during warming; (b) The field-cooled moment measured during warming (with a rate of about 0.1–0.5 K/min) after fast cooling from a temperature of 100 down to 10 K with an average rate of 3–4 K/min (solid circles); open circles mark the zero-field-cooled moment measured during warming; (c) Comparison of the field-cooled moment measured versus temperature after fast cooling down to 10 K (solid circles) with that measured during slow cooling (open circles).

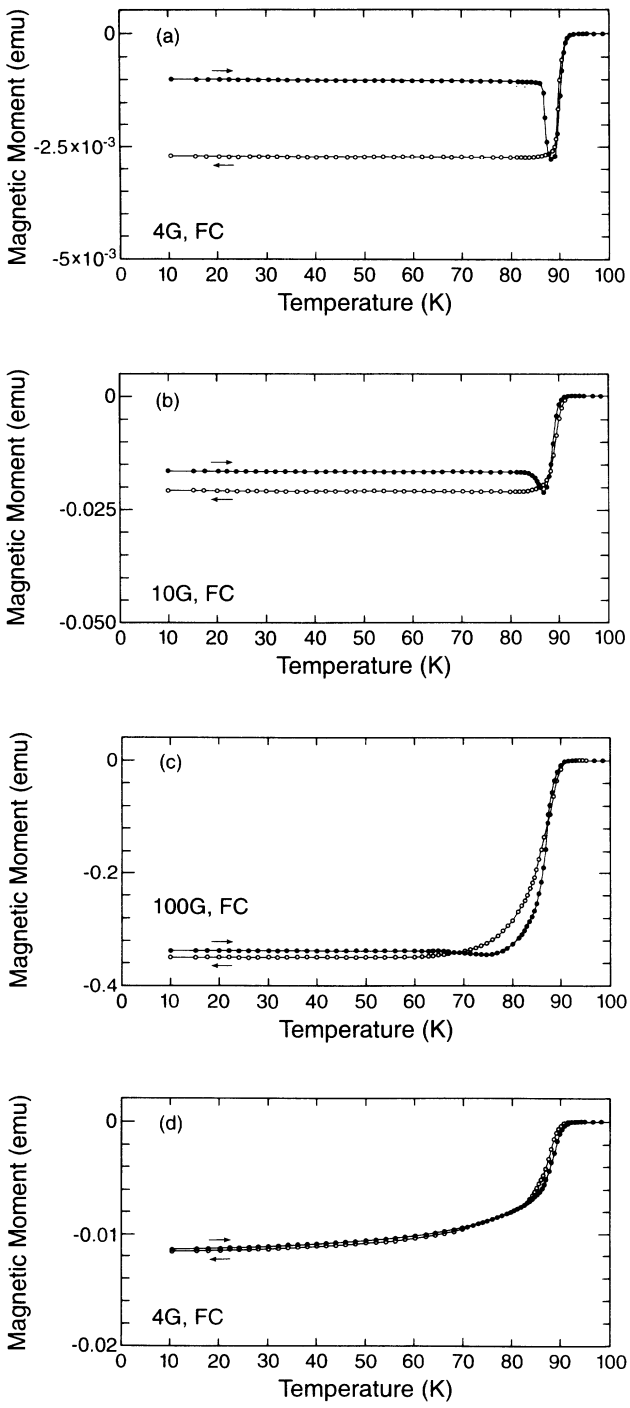

FIG. 2. Field-cooled magnetic moment measured as a function of temperature in the sample YBCO no. 2. The measurements were taken during slow cooling with a rate of 0.05–0.1 K/min (open circles) and during warming after fast cooling down to 10 K with a rate of 3–4 K/min (solid circles) at magnetic fields of 4, 10, and 100 G. The arrows indicate the change in temperature during the measurement (warming or cooling). The lines provide a guide for the eye. (a)–(c) The results obtained for the ceramic rod-shaped sample (4.5 mm in diameter and 8 mm in length). (d) The results obtained for the pressed-powder sample at 4 G (of the same dimensions as the ceramic one) formed under a pressure of 7000 bar after pulverizing (grain size, 1–5 μm) the ceramic sample.

conducting ceramic ring. Field cooling of the ring down to temperatures below T_c results in a Meissner expulsion which can be measured by the Hall probe traveling across the sample. The magnitude of the Meissner field in the ring's center was determined as a function of temperature for the fast and slow cooling procedures with cooling rates of about 0.5 and 0.05 K/min, respectively. The change in this field vs temperature allowed us to specify the amount of additional intergrain flux trapped in the ring during fast cooling, and the temperatures at which this flux was depinned. The same ring was then used to measure the dependence of the intergrain critical current on temperature for both the fast and slow field-cooling procedures. The critical current was determined by inducing a persistent current in the field-cooled ring, followed by estimation of its critical value and dissipation from measurements of the saturation and relaxation of the magnetic field generated by the current. Changes in the critical current and its decay were compared with corresponding changes in the Meissner field.

III. EXPERIMENTAL RESULTS

The measurements of the intergrain-flux trapping and its depinning were done with a SQUID magnetometer on cylinder-shaped and pellet-shaped samples of YBCO ceramics and YBCO/Ag (2 and 4 wt %) composites, and with a scanning Hall-probe system on a ring-shaped sample of YBCO/Ag (2 wt %) composite.

A. dc magnetization (SQUID) measurements

We measured the dependence of the dc magnetic moment in field-cooled YBCO and YBCO/Ag ceramic superconductors on temperature (over a range between 10 and 95 K), magnetic field (over a range between 0 and 2 kG), and time (relaxation rates measured for times up to 10^4–10^5 sec). Figure 3 shows the dependence of the magnetic moment on temperature measured for various magnetic fields (between 10 and 70 G) in ceramic YBCO, after the fast cooling procedure (cooling down to 10 K) was applied to the sample. The temperature at which the intergrain flux starts to depin decreases with increasing applied magnetic field. Depinning of the intergrain flux, trapped during fast cooling at very low magnetic fields of 1.5, 2, and 3 G, revealed that the fraction of the trapped intergrain flux which was expelled from the sample close to T_c decreases with decreasing applied field. Fast cooling of the YBCO ceramic sample down to temperatures close to T_c reduces the amount of trapped intergrain flux (Fig. 4), but it has little effect on the intergrain-flux depinning temperatures. The dependence of the Meissner moment on time was measured in YBCO for both the fast and slow cooling procedures in magnetic fields of 5 and 100 G. For the fast cooling, we found that close to T_c

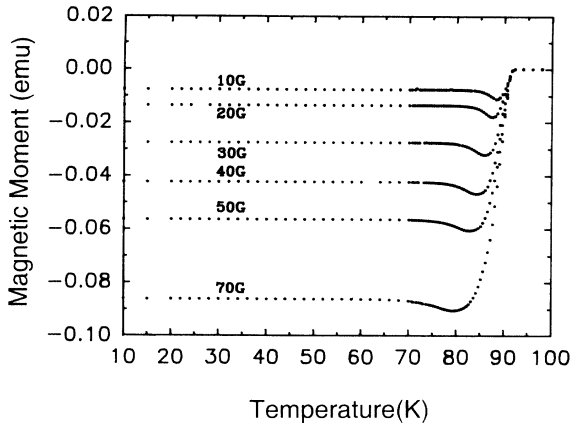

FIG. 3. Dependence of the field-cooled magnetic moment on temperature for the ceramic sample YBCO no. 3 (4.5 mm in diameter and 3.5 mm thick) which was subjected to the fast cooling procedure at various magnetic fields between 10 and 70 G. Note the shift of the intergrain-flux depinning temperature to low temperatures at higher magnetic fields.

the Meissner moment increases with time (Fig. 5) and its logarithmic increase rate depends on temperature. Such a dramatic change in the Meissner-moment increase rate was not observed for slow (equilibrium) cooling. For the fast cooling, the temperatures at which the maximum Meissner increase rate occurs correspond to those at which the maximum Meissner moment is detected (which is 87.5 K for 5 G and 71–73 K for 100 G). The measurements of the magnetic moment of the fast-cooled YBCO during subsequent warming revealed two characteristic temperatures which indicate the change in the Meissner moment (Fig. 3). The lower temperature (the "onset" temperature) determines the beginning of that change. The higher one (the "completion" temperature) corresponds to the maximum Meissner moment measured during the warming process. The onset temperature was estimated as the temperature at which the change in the Meissner moment M is more than about 3–5% of the difference $M(10\text{ K})-M(T_{\text{completion}})$. This imposes an error of about $\pm 1-2$ K on the value of this temperature.

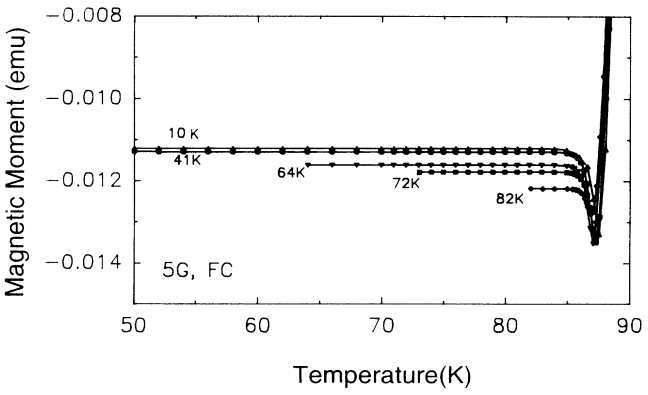

FIG. 4. Field-cooled magnetic moment measured as a function of temperature in the ceramic sample YBCO no. 1, which was subjected to the fast field-cooling procedure at 5 G. The measurements of the magnetic moment were taken during warming after fast cooling from a temperature of 100 K down to various temperatures between 10 and 82 K. Note that cooling the ceramic sample down to temperatures close to T_c reduces the amount of trapped intergrain flux. The lines provide a guide for the eye.

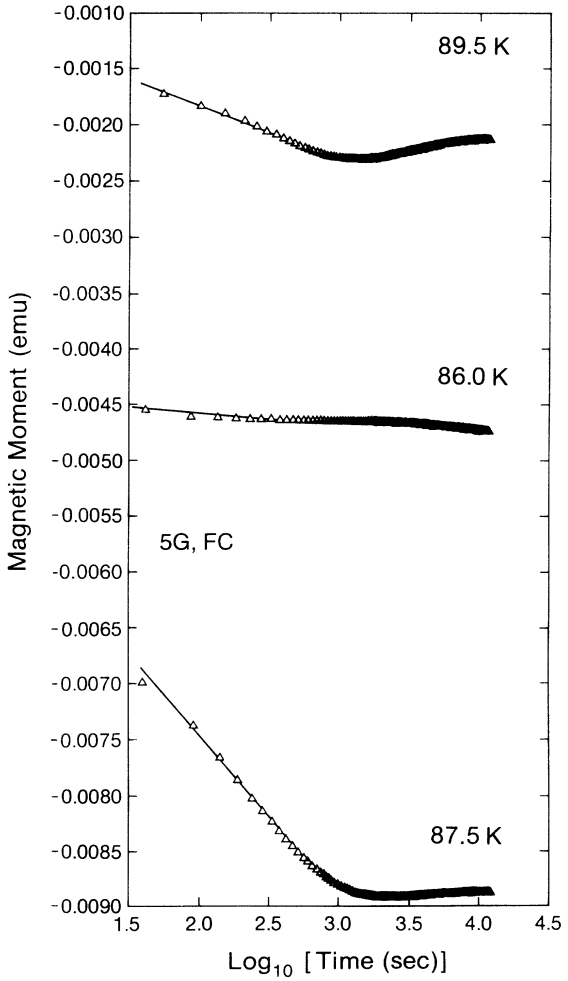

FIG. 5. Field-cooled magnetic moment measured as a function of time in the ceramic sample YBCO no. 1 at 5 G for various temperatures below T_c. The increase of the Meissner moment in the field-cooled ceramic rod at 5 G as a function of time is plotted for three different temperatures. The measurements were done during warming to the temperature of the measurement after fast cooling from 100 down to 10 K. Note that 87.5 K corresponds to the maximum Meissner expulsion. The initial change in the Meissner moment is logarithmic in time up to about 10^3 sec.

The onset and completion temperatures were found to decrease if the applied magnetic field increases. The dependence of these two temperatures on magnetic field for YBCO ceramic samples is shown in Fig. 6. At very low magnetic fields below 5G, the completion temperatures approach a constant value.

The temperatures and magnetic fields which characterize intergrain-flux depinning for YBCO/Ag (2 wt %) ceramic composites are shown in Fig. 7. The onset and completion temperatures at low magnetic fields are highest for YBCO ceramics. The completion temperatures for the YBCO/Ag (4 wt %) composite are essentially the same as those measured for YBCO/Ag (2 wt %) in magnetic fields above 25G; however, the onset temperatures are about 10 K higher than those for YBCO/Ag (2 wt %) composites.

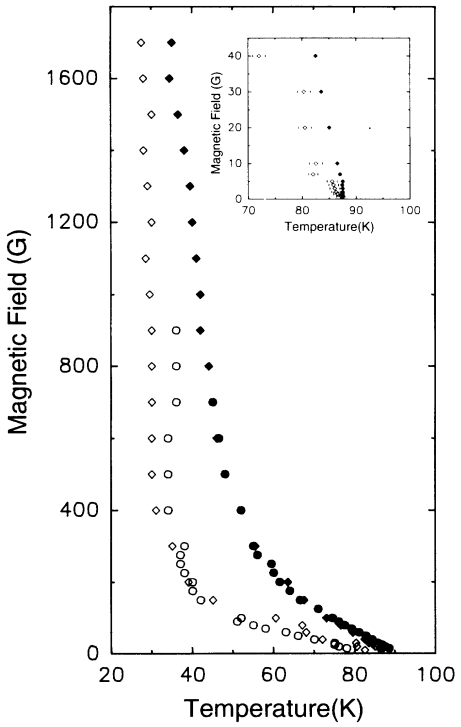

FIG. 6. Magnetic fields and temperatures which characterize intergrain-flux depinning in the ceramic samples YBCO no. 1 and no. 3 after the fast cooling procedure. Diamonds and circles represent the results for YBCO no. 1 and YBCO no. 3, respectively. Sample no. 1 is a cylinder of 4.5 mm in diameter and 10.7 mm in length. Sample no. 3 is a pellet of 4.5 mm in diameter and 3.5 mm thick. We could not detect any changes in the Meissner expulsion measured over a temperature range 10–100 K after fast cooling in fields higher than 1700 G for sample no. 1 and higher than 900 G for sample no. 3. Open and solid symbols denote temperatures and magnetic fields of the onset and completion of the intergrain-flux depinning, respectively. Note the good reproducibility of the results at low magnetic fields, up to 400 G. At high fields, discrepancy between onset temperatures for samples no. 1 and no. 3 could be caused by sample geometry. Inset: The corresponding low-field results for YBCO no. 1. Note the independence of the "completion" temperature on magnetic fields less than 5 G.

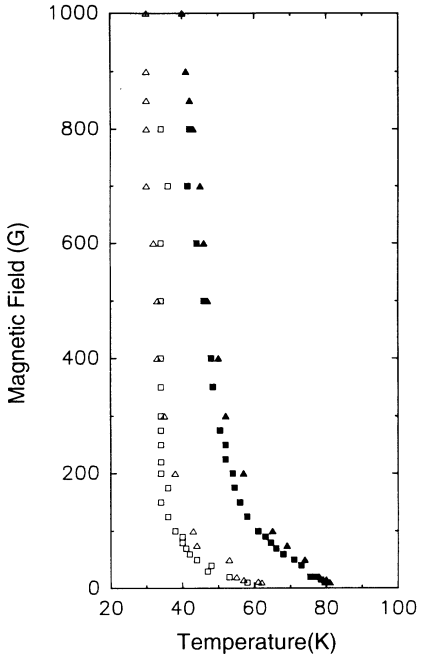

FIG. 7. Magnetic fields and temperatures which characterize intergrain-flux depinning after the fast cooling procedure in the ceramic composites of YBCO/Ag (2 wt %) no. 1 and no. 2 (represented by triangles and squares, respectively. The samples are pellets of 4.5 mm in diameter and 3.5 mm thick. The open and solid symbols denote temperatures and magnetic fields of the onset and completion of the intergrain-flux depinning, respectively.

B. Meissner-field and critical-current (Hall-probe) measurements

We performed measurements of the Meissner-field profiles across the superconducting ceramic ring of a YBCO/Ag (2 wt %) ceramic composite. The sample was either cooled fast or cooled slowly in a magnetic field. It was observed that the change in the Meissner field as a function of temperature measured above the ceramic ring [Fig. 8(a)] is qualitatively the same as that found by dc magnetization measurements [Figs. 2(a), 2(b), and 2(c)]. Our measurements revealed a corresponding change in the transport critical currents estimated from the saturation value of the persistent current induced in the ceramic ring. The superconducting ring exhibits higher critical currents for the slow-field-cooling regime in comparison to those measured for the fast cooling procedure [Fig. 8(b)]. This happens in the temperature range where the intergrain-flux depinning occurs. The sensitivity of the method allowed us to observe changes in the Meissner field and critical currents in applied fields above 20 G. We could not detect any Meissner-field changes at fields lower than 20 G.

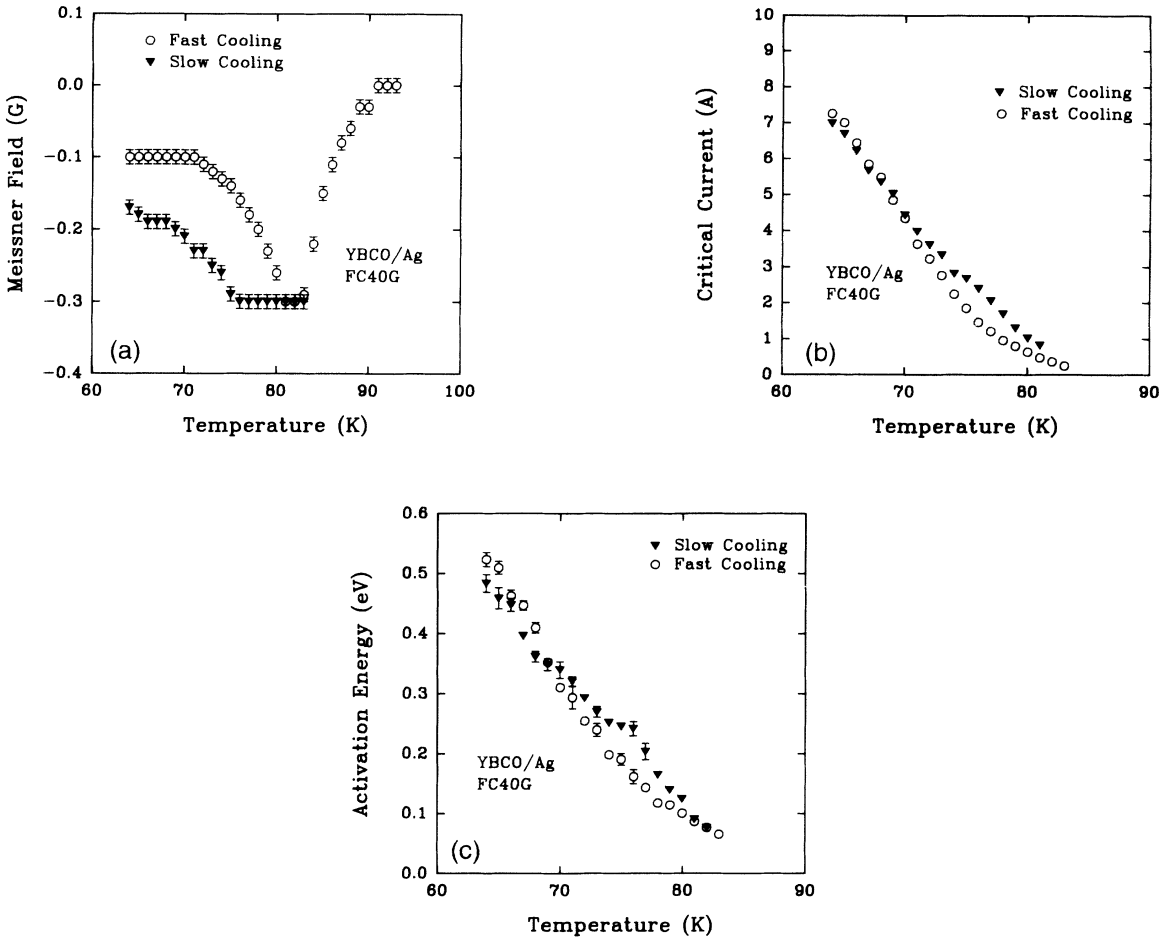

FIG. 8. (a) Temperature dependence of the Meissner field measured (using a Hall-probe system) in the center of a YBCO/Ag (2 wt %) ceramic ring-shaped sample (no. 2) cooled in a field of 40 G. For the fast cooling procedure, the data (open circles) were taken during warming after fast cooling (with a rate of 0.5 K/min) from a temperature of 95 down 64 K. For the slow cooling procedure, the data (solid triangles) were recorded during slow cooling (with a rate of 0.05 K/min) from a temperature of 83 down to 64K. The difference in the Meissner field at temperatures below 83 K is caused by the extra intergrain-flux trapping at 64 K (after fast cooling to this temperature) and subsequent depinning at temperatures higher than 71 K. (b) Temperature dependence of the critical current in the ring-shaped sample YBCO/Ag (2 wt %) no. 2 subjected to the fast and slow cooling procedures at 40 G. The measurements were performed by inducing a persistent current (up to its critical value) in the ring right after the measurement of the Meissner field, and detecting the magnetic field generated by the current with a Hall probe. Note a decrease in the critical current for the fast cooling procedure, caused by the intergrain-flux depinning. The "apparent" critical current density J_c (which is equal to the critical current I_c divided by the cross-sectional area of the sample) could be calculated according to the formula J_c (A/cm^2)$=I_c$ (A)$\times 30$/cm^2. Note that the real critical current density must be higher since the total grain-boundary area available for the supercurrent conduction is much less than the sample's cross-sectional area. (c) Temperature dependence of the activation energy for the intergrain flux creep at 40 G determined from measurement of the persistent-current dissipation. Higher activation energy corresponds to higher magnitude of the critical current.

IV. DISCUSSION

The effect of Josephson weak links on the electromagnetic properties of the superconducting ceramics (including Josephson magnetic-flux penetration and pinning), has been discussed by Clem,[19] and Tinkham and Lobb.[3] Formulas were given for the intergrain penetration depth λ_j, the intergrain coherence length ξ_j, and for the lower and upper Josephson critical fields H_{c1j} and H_{c2j}, respectively, derived in terms of λ_j and ξ_j. It was suggested that penetration of Josephson vortices along the junction depends on their pinning within that junction, which can arise either from discreteness of the Josephson-junction array or from inhomogeneity of the junction coupling strengths. Mee *et al.*[20] calculated the dependence of the Josephson-flux-creep rate on temperature. The results were achieved from an analysis of the thermally activated motion of magnetic-flux lines through a network of superconducting grains connected by Josephson junctions with potential barriers corresponding to the differences

between the minima and maxima of the function

$$U(\Delta\varphi)=-(\Phi_0/2\pi)(I_c\cos\Delta\varphi+I\Delta\varphi)\ ,$$

where I_c is the maximum Josephson current and $\Delta\varphi$ the phase difference across the Josephson junction. A relation between the transport critical current density and logarithmic flux-creep rate was derived for this model, leading to a logarithmic decay rate of transport current density. The measurements of the transport critical currents derived from the saturation value of the persistent current flowing in ceramic rings of YBCO/Ag composites revealed the decay of the current and its logarithmic dependence on time with an energy barrier proportional to the critical current I_c (Ref. 18). That information, however, did not provide a complete picture of the relationship between the Josephson-flux motion and the intergrain critical current density. The present work reveals that, under certain conditions, the Josephson-vortex motion and pinning can be separated from the intragrain-vortex motion, and that the Josephson-flux motion affects the magnitude and dissipation rate of the transport critical current density. The measurements of dc magnetic moment exhibits characteristics of the Josephson-flux motion in YBCO ceramics and YBCO/Ag ceramic composites. On the other hand, measurement of the Meissner-field profiles across a ring-shaped sample of YBCO/Ag ceramics and measurement of the critical value of the persistent current flowing in that ring, indicate directly a relationship between the transport critical current dissipation and the Josephson-(intergrain-) flux pinning. dc magnetization measurements helped us to understand the nature of the intergrain-flux trapping and depinning. When a ceramic superconductor is cooled slowly down to temperatures below T_c in a magnetic field, the Meissner currents cause a partial expulsion of the intergrain flux from the sample [Fig. 1(a)], resulting in an almost uniform distribution of the trapped flux across the sample. During fast cooling of the sample in the same magnetic field, the sample surface is cooled faster than the sample interior. The result is that initially the Meissner currents are built up on the surface while the bulk of the sample remains in the normal state and contains a large amount of magnetic flux. During fast cooling, the sample behaves more like a superconducting ring whose inner hole diameter decreases continuously with time. The Meissner currents flowing on the outer and inner surfaces of this model ring expel the magnetic flux outside the ring and into the ring's inner hole [Fig. 9(a)]. The Meissner currents cause a concentration of intergrain flux in the sample center and therefore are not able to remove the same amount of intergrain flux as during the slow (equilibrium) cooling [Figs. 1(b) and 1(c)]. As a consequence, the axial component of the intergrain flux (parallel to the external field) will form a gradient across the sample. This gradient has a higher value than that for slow cooling [Fig. 9(b)]. The gradient is supported by the Meissner currents. Because of the higher density of flux between the grains in the sample center, the motion of the individual vortices is very limited, and flux creep could occur via collective jumps of large flux bundles. The activation energy is higher for flux-bundle creep than for a single flux jump. This consequently maintains a steep intergrain-flux gradient across the sample, and at low enough temperatures, prevents intergrain-flux motion out of the sample. However, warming the sample up to temperatures close to T_c causes a gradual depinning of the intergrain flux (Fig. 3) over a broad range of temperatures. Such behavior could indicate a wide range of effective activation energies for intergrain-flux creep. This could result not only from variable coupling strength of the intergrain junctions but also from the variable size of the intergrain-vortex bundle.

The amount of intergrain flux which was trapped during fast cooling (and subsequently depinned during warming) increases with the applied magnetic field (Fig. 3), reaches a maximum at magnetic fields between 100 and 500 G, and decreases for magnetic fields higher than about 500 G. The reduction of this amount at applied magnetic fields above 500 G could be caused by partial decoupling of the grains at those fields.

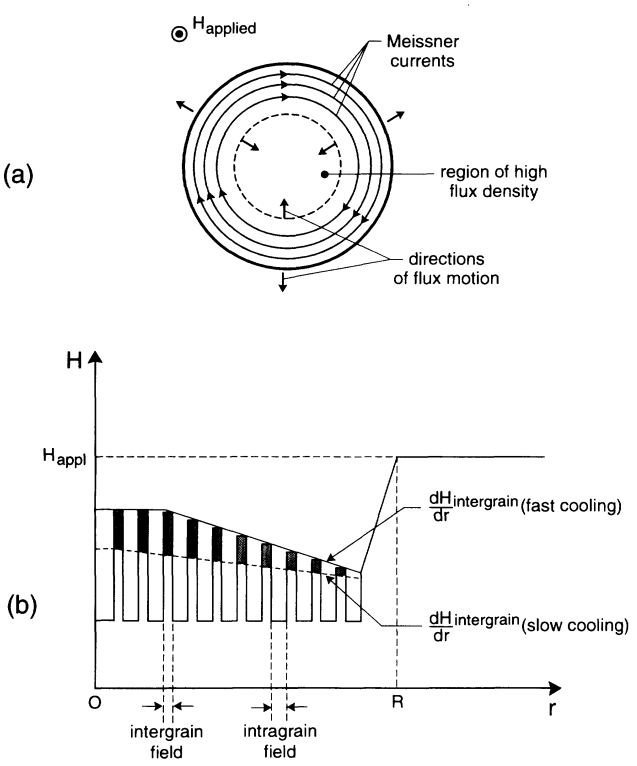

FIG. 9. (a) Schematic illustration of the intergrain-flux trapping mechanism in the ceramic cylinder of a high-temperature superconductor which was subjected to fast cooling in an applied magnetic field. The direction of the magnetic field is parallel to the cylinder axis. During fast cooling, due to the low thermal conductivity of a ceramic superconductor, the sample surface is cooled faster than its interior. Therefore, the Meissner currents will build up on the surface, pushing the intergrain magnetic flux inside the normal region at the sample center. (b) Schematic illustration of the intergrain-flux gradient steepening by the fast field-cooling procedure described in (a). R denotes the radius of a cylindrical sample.

The temperature to which a ceramic sample is cooled quickly down in a magnetic field affects the amount of intergrain flux trapped during the cooling process (Fig. 4). The trapping is less effective for temperatures closer to T_c. At those temperatures, the Meissner currents, which are responsible for trapping the excess intergrain flux at the sample center [Fig. 9(b)], are not as strong as those at a temperature of 10 K, and, therefore, one should expect a reduction of the intergrain-flux amount in the sample. The intergrain flux trapped during the fast cooling procedure is expelled from the sample when its temperature is raised (Fig. 3) above a certain temperature called the "onset temperature." The process of flux expulsion occurs gradually over a wide temperature range which depends on magnetic field. The rate at which the intergrain flux is removed from the sample depends on temperature (Fig. 5) and magnetic field. The flux expulsion occurs with a maximum rate at a temperature called the "completion temperature," which corresponds to the maximum Meissner moment. The onset and completion temperatures decrease in an increasing applied magnetic field. These temperatures, and the corresponding fields are plotted in Figs. 6 and 7 for various cylinder- and pellet-shaped samples of YBCO ceramics and YBCO/Ag (2 wt %) ceramic composites. It is observed as a general trend that the difference between the onset and completion temperatures increases rapidly with magnetic field, reaching a maximum at fields between 200 and 400 G, and then decreases very slowly at higher magnetic fields. The change in magnetic field from 0 up to about 200–400 G reduces the onset temperature by about 40–50 K. At higher fields, this temperature reaches an approximately constant value of about 30 K. The completion temperatures, however, exhibit slow linear reduction in magnetic fields higher than 200–400 G, for all cases studied. Figures 6 and 7 show good reproducibility of the values of the onset and completion temperatures determined for various samples of YBCO or YBCO/Ag (2 wt %) ceramics. These measurements were performed on samples of similar cylindrical geometry, i.e., 4.5 mm in diameter and 3.5–8.0 mm in length. Modification of the intergrain pinning at junctions in YBCO ceramics can be realized by adding small amounts of silver (2–4 wt %) during the sintering process of YBCO. This causes not only improvement of the intergrain contacts and consequently enhancement of the intergrain critical current but also reduction in the number of intergrain-magnetic-flux pinning centers, and in the energy barrier for intergrain-flux creep (Ref. 18). At low magnetic fields up to about 100 G, YBCO and YBCO/Ag (2 wt %), materials are characterized by the strongest and the weakest intergrain-flux pinning, respectively. The samples for which this comparison was made were cut out of the center of disk-shaped samples (16 mm in diameter and 3.5 mm thick). The remaining ring-shaped samples were used for the critical-current studies. Persistent currents induced in those rings were applied to estimate the critical-current value and its dissipation. The highest current decay rates were recorded in the YBCO/Ag (2 wt %) composite and the lowest ones in the YBCO ceramic. On the other hand, the highest critical current values were detected in YBCO/Ag (2 wt %) composite and the lowest ones in YBCO ceramic. Therefore, low onset temperatures for the intergrain-flux depinning imply high dissipation rates of the transport current.

We attempted to correlate the measurements of the intergrain-flux depinning with the measurements of critical-current magnitude and its dissipation. In order to make such a correlation reliable, i.e., independent of the sample geometry and measurement method, all the studies were performed on the same ring-shaped sample and with the same technique (a scanning Hall-probe system). Due to the sensitivity limit of the system, we were able to detect changes in the intergrain-flux trapping and corresponding changes in the critical current only in samples of the ceramic YBCO/Ag (2 wt %) composite (which was characterized by the lowest intergrain-flux pinning barrier and the highest current dissipation rates) and only for magnetic fields higher than about 20 G.

The results are shown in Fig. 8. The changes in Meissner expulsion measured as a function of temperature in the center of the ceramic ring, which was subjected to the fast and slow cooling procedures at a magnetic field of 40 G, reveal similar features to the corresponding changes in magnetic moment measured with a dc SQUID magnetometer. Note that the onset and completion temperatures at 40 G for the ring-shaped sample [Fig. 8(a)] are higher than those measured at 40 G in the sample cut from the center of this ring (Fig. 7). The reason for that is the sample geometry. It was previously reported that the effective activation energy for intergrain-flux creep in YBCO ceramics depends on sample geometry, and suggested that intergrain-flux gradients are a possible cause for the change in this energy (Ref. 4). The effective activation energy was observed to decrease when sample dimensions were reduced. Cooling a ring-shaped sample of YBCO/Ag (2 wt %) down to 64 K from a temperature of 95 K above T_c with a rate of about 0.5 K/min results in additional flux being trapped at the grain boundaries and consequently in reduction of the Meissner expulsion (see Fig. 8(a); fast cooling). Subsequent warming of this sample results in the intergrain flux being partly depinned at temperatures between 70 and 82 K. Slow cooling (with a rate of about 0.05 K/min) of the same sample causes less intergrain-flux trapping than fast cooling. Depinning of the intergrain flux which was trapped during the fast cooling procedure affects the critical value of the persistent current induced in the ring [Fig. 8(b)]. The persistent current was found to decay logarithmically with time from its maximum value. Dissipation of this current is caused by intergrain-flux creep. The activation energy E for intergrain-flux motion was calculated using the formula

$$\frac{1}{I_c}\frac{dI}{d\ln t} = -\frac{kT}{E} .$$

Higher activation energy corresponds to higher magnitude of the critical current [Fig. 8(c)]. Note that the changes in the activation energy appear to be proportional to those in the critical current.

Note that temperatures T_{cj} at which the intergrain critical current drops to zero are about 1°–2° higher than

the "completion" temperatures at which the Meissner expulsion reaches its equilibrium value (Fig. 8). This may indicate that the dependence of the completion temperature on magnetic field represents that of T_{cj} on magnetic field. For pure YBCO, the completion temperatures are proportional to the magnetic fields over a range up to about 100–150 G (Fig. 6). T_{cj} is also proportional to H, as determined from measurements of the intergrain critical current versus temperature for various magnetic fields (0–30 G) using persistent currents circulating in a ceramic ring (Ref. 18).

In order to facilitate discussion of the effects of granularity on the superconducting properties of high-temperature superconductors, Tinkham and Lobb[3] and Clem[19] adopted a simplified model of a granular material as a three-dimensional array of cubic grains connected by Josephson junctions of coupling energy $E_j=\hbar I_c/2e$, where I_c is the associated junction critical current. Such an array is able to pin the intergrain magnetic flux if an inhomogeneity of E_J exists in the medium. In polycrystalline YBCO superconductors, the grain boundaries act as Josephson tunnel junctions and the transport critical current I_c through the sample can be treated as the average Josephson current across grain boundaries. The magnetic-field dependence of the average current per junction can be approximated by an envelope function of Fraunhofer-like pattern,[19,21]

$$I_c(H)=I_c(0)\left|\frac{\sin(\pi\Phi/\Phi_0)}{\pi\Phi/\Phi_0}\right|, \tag{1}$$

where $\Phi=HA_j$ and A_j is the effective field-penetrated junction area. The temperature dependence of the critical current is linear at temperatures close to the junction critical temperature T_{cj}:

$$I_c(T)=I_c(0)\left[1-\frac{T}{T_{cj}}\right]. \tag{2}$$

Measurements of the critical current versus temperature in YBCO for various magnetic fields over a range 0–30 G (Ref. 18) showed that the linear temperature dependence of I_c is preserved at those fields. Therefore, one can separate the magnetic-field and temperature dependence of the average I_c per junction into two separate factors:

$$I_c(T,H)=I_{c0}\left[1-\frac{T}{T_{cj}}\right]\left|\frac{\sin(\pi H/H_0)}{\pi H/H_0}\right|_{\rm env}, \tag{3}$$

where I_{c0} is the critical current at $T=0$, and $H=0$.

According to the arguments given by Lobb, Abraham, and Tinkham[22] and van der Zant *et al.*,[23] the motion of the intergrain magnetic vortices in the Josephson-junction array can be thermally activated with an energy barrier equal to $U_0=\gamma E_j$, where the constant $\gamma<1$ depends on the array geometry, and E_j is the average coupling energy per junction. Using expression (3) the barrier can be written as

$$U_0(T,H)=\gamma E_{j0}\left[1-\frac{T}{T_{cj}}\right]\left|\frac{\sin(\pi H/H_0)}{\pi H/H_0}\right|_{\rm env}, \tag{4}$$

where E_{j0} is the coupling energy at $T=0$, and $H=0$.

For magnetic fields higher than about 20–30 G close to T_{cj}, the barrier U_0 can be approximated by:[24]

$$U_0(T,H)=\gamma E_{j0}\left[1-\frac{T}{T_{cj}}\right]\frac{H_0}{|H|+H_0}. \tag{5}$$

A current flowing through Josephson junctions causes a reduction of U_0 by a factor proportional to the Lorentz force density F_L, i.e., by $F_L VX$, where V is the vortex volume and X the geometrical width of the energy barrier.

Very close to T_{cj}, $U_0\simeq kT_{cj}$ and it therefore appears

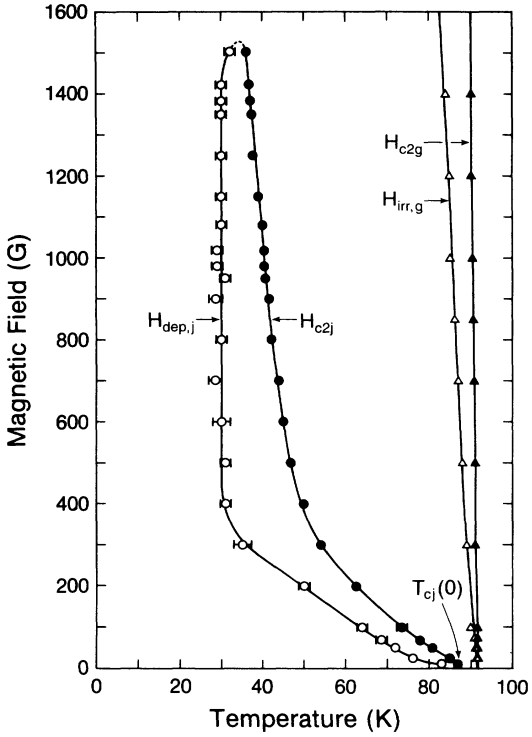

FIG. 10. Schematic representation of the intergrain- and intragrain-flux pinning and depinning regions at low magnetic fields. Indices g and j mark the intragrain and intergrain properties, respectively. T_{cj} and H_{c2j} represent temperatures and magnetic fields at which the Josephson (intergrain) current drops to zero [$T_{cj}(0)$ stands for T_{cj} at zero magnetic field]. The curve marked $H_{dep,j}$ represents the onset of intergrain-flux depinning. The data which characterize the intergrain-flux depinning are those taken for the ceramic sample YBCO no. 2. Open circles denote the temperatures and magnetic fields of the onset of depinning. Solid circles mark the temperatures and magnetic fields at which depinning occurs with the maximum rate (see Fig. 5). Those symbols virtually coincide with temperatures and magnetic fields at which the superconducting grains are decoupled. Open and solid triangles represent the irreversibility line and the upper critical field measured in the pressed-powder sample (which was produced after pulverizing the ceramic YBCO no. 2 sample). The irreversibility line is characterized by temperatures and magnetic fields at which the zero-field-cooling and field-cooling magnetic moments coincide.

that the dependence of T_{cj} on magnetic field is determined by that of the Josephson critical current [with a $\sin H/H$ factor in Eq. (4)]. Note that the dependence of the intergrain-flux depinning temperatures on magnetic field (Figs. 6 and 7) resembles that of I_{cj} on magnetic field. A representation of various regions of the intergranular and intragranular flux pinning in granular high-temperature superconductors (based on the experimental data for the YBCO no. 2 sample) is shown in Fig. 10. The curve marked H_{c2j} represents the change of the grain-decoupling field with temperature or the change in the intergrain critical temperature T_{cj} with magnetic field. The curve marked $H_{\mathrm{dep},j}$ represents the onset of intergrain-flux depinning (and the corresponding decrease in the intergrain critical current density). $H_{c2j}(T)$ coincides with temperatures and magnetic fields at which the intergrain-flux depinning occurs with the maximum rate (Fig. 5). Weak Josephson-flux pinning, which was observed in YBCO/Ag (2 wt %) composites, will shift the $H_{c2j}(T)$ and $H_{\mathrm{dep},j}(T)$ lines (over a range of field between 10 and 400 G) down to low temperatures.

V. CONCLUSIONS

Studies of the Josephson-flux motion and corresponding dissipation of the Josephson critical current in the Josephson-junction network of high-T_c granular superconductors require special experimental techniques. These techniques must ensure that:

(i) measurements of the Josephson-flux properties are performed without the influence of the intragrain (Abrikosov) flux;

(ii) the measurements represent a true response of the transport critical current, flowing through the Josephson-junction network, to the motion of the Josephson vortices.

The methods that satisfy the above requirements are:

(i) dc magnetization measurements of the Meissner moment of granular high-T_c superconductors subjected to fast and slow field-cooling procedures;

(ii) contactless detection of the critical-current magnitude and dissipation using persistent currents induced in field-cooled ceramic rings and corresponding measurement of the Meissner field.

The former technique was applied to measure the magnetic properties of the intergrain Josephson-junction network in YBCO and YBCO/Ag superconductors, namely, the temperatures and magnetic fields at which Josephson vortices depin, and the corresponding relaxation effects. These temperatures and magnetic fields depend on the sample geometry and the intrinsic properties of the grain boundaries. The effect of geometry is reflected through the presence of intergrain-flux gradients, which reduce the effective activation energy for intergrain-vortex motion. Modification of the grain boundaries in YBCO by adding silver during the sintering process has a pronounced effect on the intergrain-flux depinning, resulting in reduction of the pinning-barrier height and the number of strong pinning centers. This means that in general the superconductor-insulator-superconductor (SIS) junction network in YBCO is characterized by large variation in the coupling energy within the junction network, but on the other hand little variation in the coupling energy (with a large grain-boundary area available for the current conduction as shown by the earlier experiments[18]) is a characteristic of the superconductor–normal metal–superconductor (SNS) junction network in YBCO/Ag. According to the models of Josephson-junction networks in high-T_c granular superconductors developed by Tinkham and Lobb[3] and Clem,[19] the pinning barrier for the Josephson-flux motion in the junction network originates from variation of the Josephson-coupling energy $E_j = \hbar I_{cj}/2e$. The measurements of the dependence of intergrain-flux depinning temperatures on magnetic field H (Figs. 6 and 7) show that the functional dependence of those temperatures on H resembles that of $I_{cj}(H)$. Also, the changes in the effective activation energy for intergrain-flux creep (Fig. 8) correspond to those in the intergrain critical current. These observations support the above models; however, more work is required in order to determine the source of the coupling-energy variation in SIS and SNS junction networks of granular high-T_c superconductors and its relationship to Josephson-vortex motion.

We applied a technique which uses a self-sustaining supercurrent and a contactless detection of its magnitude and dissipation, in simultaneous combination with measurement of the intergrain-flux depinning, in order to study the direct relationship between depinning (and motion) of the Josephson magnetic vortices and dissipation (and magnitude) of the transport (Josephson) critical current. Such information is of primary importance for studies of the transport and magnetic properties of the Josephson-junction network. The experiments allowed detection of the Josephson-flux depinning without the influence of the intragrain flux, and simultaneous direct measurement of the intergrain critical-current magnitude and dissipation (using the same granular sample and the same measurement technique). The results also included direct detection of the changes in activation energy for the Josephson-flux motion and corresponding changes in the Josephson critical current. Such an approach is especially useful for future studies of inhomogeneities in the coupling energy within the Josephson-junction network of granular superconductors.

ACKNOWLEDGMENTS

We are pleased to acknowledge useful discussions with Professor J. R. Clem. This work was supported by grants from the Natural Sciences and Engineering Research Council of Canada (NSERC).

[1]H. Dersch and G. Blatter, Phys. Rev. B **38**, 11 391 (1988).
[2]J. F. Kwak, E. L. Venturini, P. J. Nigrey, and D. S. Ginley, Phys. Rev. B **37**, 9749 (1988).
[3]M. Tinkham and C. J. Lobb, Solid State Phys. **43**, 91 (1989).
[4]M. A.-K. Mohamed and J. Jung, Phys. Rev. B **70**, 4512 (1991).
[5]E. H. Brandt, Int. J. Mod. Phys. B **5**, 751 (1991); Physica C **185-189**, 270 (1991).
[6]R. S. Markiewicz, Physica C **171**, 479 (1990).
[7]R. J. Soulen, Jr. and S. A. Wolf, Physica C **166**, 95 (1990).
[8]K. A. Müller, M. Takashige, and J. G. Bednorz, Phys. Rev. Lett. **58**, 1143 (1987).
[9]T. T. M. Palstra, B. Batlogg, R. B. van Dover, L. F. Schneemeyer, and J. V. Waszczak, Phys. Rev. B **41**, 6621 (1990).
[10]R. H. Koch, V. Foglietti, W. J. Gallagher, G. G. Koren, A. Gupta, and M. P. A. Fisher, Phys. Rev. Lett. **63**, 1511 (1989).
[11]A. Hebard, P. Gammel, C. Rice, and A. Levi, Phys. Rev. B **40**, 5243 (1989).
[12]P. L. Gammel, L. F. Schneemeyer, J. V. Waszczak, and D. J. Bishop, Phys. Rev. Lett. **61**, 1666 (1988).
[13]M. Nikolo and R. B. Goldfarb, Phys. Rev. B **39**, 6615 (1989).
[14]R. Behr, J. Kotzler, A. Spirgatis, W. Assmus, R. Gross, and M. Schwarz, in *High Temperature Superconductors—Materials Aspects,* Proceedings of the ICMC '90 Topical Conference on Materials Aspects of High Temperature Superconductivity, edited by H. C. Freyhardt, R. Flukiger, and M. Peuckert (DGM-Informationsgesellschaft, Oberursel, 1991), Vol. 2, p. 1089.
[15]J. W. Ekin, H. R. Hart, Jr., and A. R. Gaddipatti, J. Appl. Phys. **68**, 2285 (1990).
[16]R. L. Peterson and J. W. Ekin, Phys. Rev. B **37**, 9848 (1988).
[17]J. Jung and M. A-K. Mohamed, J. Adv. Sci. (Jpn.) **4**, 50 (1992).
[18]J. Jung, I. Isaac, and M. A-K. Mohamed, Phys. Rev. B **48**, 7526 (1993).
[19]J. R. Clem, Physica C **153-155**, 50 (1988).
[20]C. Mee, A. I. M. Rae, W. F. Vinen, and C. E. Gough, Phys. Rev. B **43**, 2946 (1991).
[21]K. H. Müller and D. N. Matthews, Physica C **206**, 275 (1993).
[22]C. J. Lobb, D. W. Abraham, and M. Tinkham, Phys. Rev. B **27**, 150 (1983).
[23]H. S. J. van der Zant, F. C. Fritschy, T. P. Orlando, and J. E. Mooij, Phys. Rev. B **47**, 295 (1993).
[24]K. H. Müller, Physica C **168**, 585 (1990).

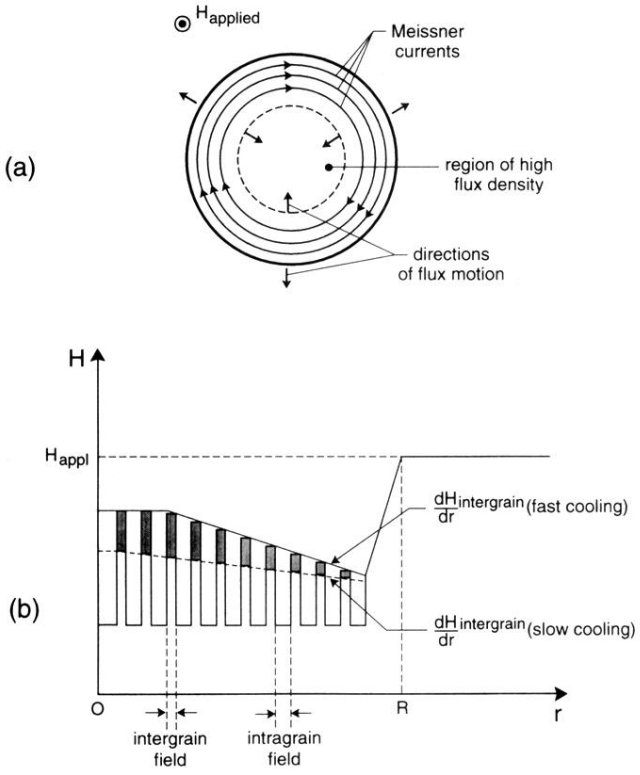

FIG. 9. (a) Schematic illustration of the intergrain-flux trapping mechanism in the ceramic cylinder of a high-temperature superconductor which was subjected to fast cooling in an applied magnetic field. The direction of the magnetic field is parallel to the cylinder axis. During fast cooling, due to the low thermal conductivity of a ceramic superconductor, the sample surface is cooled faster than its interior. Therefore, the Meissner currents will build up on the surface, pushing the intergrain magnetic flux inside the normal region at the sample center. (b) Schematic illustration of the intergrain-flux gradient steepening by the fast field-cooling procedure described in (a). R denotes the radius of a cylindrical sample.